Available online at www.sciencedirect.com
SCIENCE DIRECT®
Biochemical and Biophysical Research Communications 322 (2004) 303–309
BBRC
www.elsevier.com/locate/ybbrc

# Fluorescent intensity of a novel NADPH-binding protein of *Vibrio vulnificus* can be improved by directed evolution

Chun Chin Chang[a], Yin Ching Chuang[b], Ming Chung Chang[a,*]

[a] *Institute of Basic Medical Sciences, College of Medicine, National Cheng Kung University, Tainan, Taiwan, ROC*
[b] *Department of Medical Research, Chi Mei Medical Center, Tainan, Taiwan, ROC*

Received 6 July 2004

**Abstract**

Blue fluorescent protein, BfgV, found from *Vibrio vulnificus* CKM-1, fluoresces through augmenting the intrinsic fluorescence of bound NADPH. Random mutagenesis and DNA shuffling were applied to increase the fluorescent intensity of BfgV. The wild type *bfgV* gene was subjected to four cycles of mutagenesis processes. A prominent D7 mutant protein had fluorescent intensity four times larger than wild type BfgV. The emission wavelength of this mutant protein appeared at 440 nm, which was 16 nm shorter than that of BfgV. There were eight amino acid substitutions in D7. As these substitutions were assigned to the modeled 3D structure of BfgV, three of them, V83M, G176S, and E179K, were shown to be located around NADPH-binding site. Time course analysis indicated the synthesis of D7 protein and fluorescent expression in *Escherichia coli* transformants were synchronic. This property was different from that of wild type GFP.


*Keywords:* BfgV; Directed evolution; Fluorescence; Modeling; NADPH; Short chain dehydrogenase/reductase superfamily; *Vibrio vulnificus*

Green fluorescence protein (GFP) is known as a popular tool in molecular biology. Various experiments have been applied to enhance the fluorescent intensity of GFP [1–3] or to change its green fluorescent color to red or blue [4,5]. These fluorescent variations are mostly due to the minor changes around or just in a special fluorophore structure in this protein molecule. Besides GFP, there is another kind of fluorescent protein, which fluoresces through binding a fluorescent cofactor such as NAD(P)H [6–8]. As described in our previous report, a fluorescent protein gene, *bfgV*, cloned from *Vibrio vulnificus* CKM-1, made transformed *Escherichia coli* cells fluoresce as excited by long wavelength ultraviolet [9,10]. Our study also showed the fluorescence of BfgV–NADPH complex mainly resulted from the amplification of intrinsic fluorescence of bound NADPH by BfgV apoprotein [9]. Although some proteins can alter the intrinsic fluorescent intensity and emission wavelength of bound NAD(P)H, the levels of these variations are different from one protein to another. Estradiol 17β-dehydrogenase amplifies four times the intrinsic fluorescent intensity of bound NADPH and shifts its emission wavelength from 457 to 436 nm [8]. The fluorescent intensity of bound NAD(P)H on malate enzymes is 2–3 times larger than that of free form NAD(P)H, and the emission wavelength shifts from 465 to 440 nm or remains unchanged [6,7]. However, the increase of fluorescence is not universal in all NAD(P)H-binding proteins because there is at least one exception, glyceraldehyde-3-phosphate dehydrogenase [11]. The fluorescent increase of bound NAD(P)H is proposed to be the result of its conformational change by the interaction with protein [11]. Therefore, it may be possible to increase the fluorescent intensity of a protein–NAD(P)H complex by fine-tuning its protein skeleton. Because BfgV is the first fluorescent protein found in marine-borne *V. vulnificus* and also the first

* Corresponding author. Fax: +886 6 2754697.
*E-mail address:* mcchang@mail.ncku.edu.tw (M.C. Chang).

0006-291X/$ - see front matter © 2004 Elsevier Inc. All rights reserved.
doi:10.1016/j.bbrc.2004.07.117

NADPH-binding protein making *E. coli* transformants emit naked-eye detectable fluorescence, we considered this protein is worth to be a good model to study this ratiocination.

Up to now, various promising mutagenesis strategies have been developed to effectively direct proteins to change their features toward specific requirements [2,12–14]. These strategies are generally called directed evolution [15]. Many impressive and successful cases have been reported in the past, such as subtilisin E [16,17] by error-prone PCR [13]; β-lactamase [18], β-galactosidase [19], and GFP by DNA shuffling [2]; paranitrobenzyl esterase by both error-prone PCR and DNA shuffling [20]; and thymidine kinase by cassette mutagenesis [12,14].

In this study, we used error-prone PCR (random mutagenesis) and DNA shuffling methods to evolve *bfgV* gene, and eventually got a promising mutant *D7*. Its derived protein made significant progress in fluorescent intensity. Partial three-dimensional (3D) structure of BfgV–NADPH complex was also modeled to show the D7 mutation sites. The analytical results of protein synthesis and fluorescent formation of D7 in transformed *E. coli* cells were also showed in this report.

## Materials and methods

*Bacterial strains and growth medium.* The bacterium *V. vulnificus* CKM-1 was a clinical isolate from the Medical Center of National Cheng Kung University [9,10]. *E. coli* BL21(DE3) (Stratagene; CA, USA) was used as a host for gene expression and screening work. Bacteria used in this study were raised in Luria–Bertani (LB) broth or on LB agar. When required, ampicillin was added into the medium at 100 μg/ml except where otherwise noted. Isopropylthio-β-D-galactoside (IPTG) was used as inducer at 1 mM in broth and 0.1 mM in agar plates. All medium components were purchased from Difco (MI, USA) and chemicals were from Sigma (MO, USA).

*Plasmid construction.* A 751-bp fragment containing a complete 720-bp open reading frame (ORF) of *bfgV* and 31-bp upstream noncoding sequence was inserted into pET21b vector (Novagen; WI, USA). This recombinant plasmid was called pFP21 [9]. The *bfgV* in pFP21 replaced by its evolved mutant *D7* was designated as pD721. The plasmid pGFP (Clontech; CA. USA) containing wild type *gfp* gene which can express in *E. coli* was used to compare with p19D7 for fluorescent formation. The p19D7 plasmid was identical to pGFP except that *gfp* was replaced by *D7*.

*Random mutagenesis.* Random mutation was performed on entire *bfgV* gene by error-prone PCR [13]. A 100 μl reaction mixture contained 50 mM Tris (pH 8.3), 6.6 mM $MgCl_2$, 50 mM KCl, 0.5 mM $MnCl_2$, 200 μM dNTP mixture, 50 pmol each of oligonucleotide primer, 20 ng template DNA, and 3 U *Taq* DNA polymerase (Promega; WI, USA). Two primers, EP-F1 (5′-CTA CGC ATC TAG AAG CCA AAA CGG C-3′) and EP-R1 (5′-GTG ATA AGC TCG AGC GGT TAT GG-3′), were designed for PCR. Thermal cycling was performed with the following conditions: 1 cycle of 94 °C for 30 s; 30 cycles of 94 °C for 10 s, 60 °C for 15 s, and 72 °C for 40 s, followed by 1 cycle of 72 °C for 10 min. The PCR products were purified by QIAquick Gel Extraction Kit (QIAGEN; Hilden, Germany) and inserted into pET21b. These recombinant plasmids were then transferred into BL21(DE3) to become a *bfgV* mutant library.

*DNA shuffling.* The DNA shuffling protocol was slightly modified from Stemmer's report [21]. All 751-bp inserts in candidate plasmids were amplified by normal PCR. An equal amount of each PCR product was mixed. About 400 ng of this mixture was dissolved into 18 μl of 10 mM Tris buffer (pH 7.5) and then 2 μl of 10× DNase I digestion buffer (500 mM Tris–HCl, pH 7.5, 10 mM $MnCl_2$) was added. This DNA mixture was digested by DNase I (Sigma) for 15–30 min. DNA fragments around 50 bp were purified from 2% agarose gel and then resuspended in 50 μl PCR mixture (10 mM Tris–HCl, pH 9.0, 0.2 mM dNTP, 1.5 mM $MgCl_2$, 50 mM KCl, 0.1% Triton X-100, and 1.5 U *Taq* DNA polymerase). Primerless PCR was then carried out with the following conditions: 1 cycle of 94 °C for 40 s; 35 cycles of 94 °C for 20 s, 50 °C for 10 s, and 72 °C for 10 s, followed by 1 cycle of 72 °C for 5 min. After adequate dilution of this PCR product, 40 additional PCR cycles were performed under the existence of EP-F1 and EP-R1 primers. These reassembled fragments were cloned back into pET21b for screening.

*Mutant screen.* Transformed BL21(DE3) cells were raised on LBAI agar (LB agar containing 50 μg/ml ampicillin and 0.1 mM IPTG) at 37 °C for 16 h and then illuminated with long wavelength ultraviolet equipped in an ImageMaster VDS system (Amersham–Pharmacia; NT, HK). Colonies with fluorescence brighter than the one selected from previous round were picked out for further confirmation. All selected candidates were subjected to broth culture for fluorescent index (FI) determination. In brief, each transformant was first inoculated into 20 ml LBA broth and cultured at 37 °C for 16 h with 200 rpm shaking. Then, 0.5 ml of this overnight culture was inoculated into 50 ml LBA broth for 1.5 h cultivation. IPTG was added to induce protein synthesis and then broth was incubated for another 1.5 h. At last, cells were collected and washed three times with ice-cold 50 mM phosphate buffer (pH 7.5). Two milliliters of each well-diluted cell suspension was subjected to fluorescence determination in a Perkin–Elmer LS50B luminescence spectrometer with the excitation wavelength at 352 nm and emission wavelength at 456 nm. Fluorescent intensity normalized by $OD_{600}$ of each sample was designed as fluorescent index (FI).

*Determination of fluorescent spectra.* Transformed *E. coli* cells were raised and collected as the same way in mutant screen except the addition of IPTG at the beginning of 50 ml culture. The way of determining the fluorescent spectra of *E. coli* transformants was the same as our previous report [9].

*3D structure modeling of BfgV.* The partial 3D structure of BfgV based on the coordinates of meso-2,3-butanediol dehydrogenase (m-BD) of *Klebsiella pneumoniae* [22] was modeled by the ProModII program in SWISS-MODEL server [23–25]. Only 1–194 residues of BfgV were used for modeling while the remaining 45 residues with less similarity at C-terminal were ignored.

## Results

### *Construction of mutant library and screening bfgV mutant*

Random mutations were first introduced into *bfgV* by error-prone PCR method. About 95,000 transformants from the first mutant library were screened on plates. All selected candidates were subjected to the second step of broth culture for FI determination. One mutant, named *A48*, made the highest FI value and became the parent gene for the second round mutagenesis. In the second round work, error-prone PCR was adopted again and about 100,000 transformants were screened. Although more than 20 colonies displayed fluorescence brighter than those harboring *A48* on plates, only five mutants *B5*, *B9*, *B10*, *B13*, and *B17* made FI values

20–30% larger than their parent *A48*. In the third round, DNA shuffling was applied to collect potentially beneficial mutations into a single gene. The five B-series mutant genes were used as parents for DNA shuffling and the wild type *bfgV* was also included to remove noxious mutations. Three recombinant genes, *C8*, *C9*, and *C13* selected from this process, had FI values slightly greater than the five B-series parents. Their deduced amino acid sequences revealed that these three mutants indeed contained chimera mutation patterns that were different from their five parents. Lastly, we returned to use random mutagenesis for the fourth round work. We mixed equal amount of *C8*, *C9*, and *C13* DNA as the parents to extend genetic background and to avoid losing any promising lineage. One mutant, *D7*, selected from this cycle made the highest FI value, four times larger than wild type *bfgV*. Fig. 1 summarized the residue substitution sites of D7 and its direct progenitors, while Fig. 2 illustrated their relative FI values. The fluorescent colonies expressing wild type BfgV or D7 mutant protein are shown in Fig. 3.

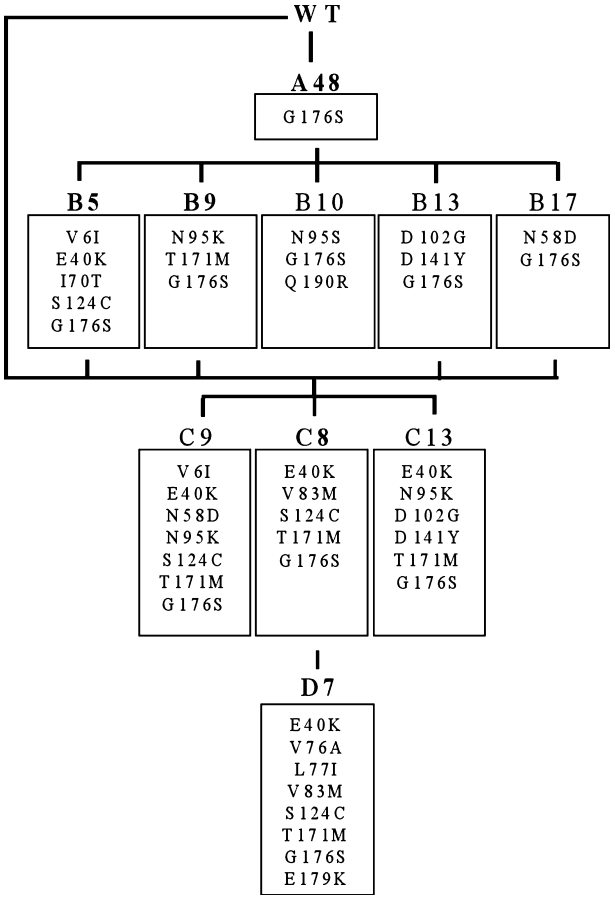


Fig. 1. Lineage of D7 mutant generated by directed evolution. Amino acid substitutions of progressive candidates selected from each round are listed in individual rectangular block. The name of each mutant is labeled on top of each block. The boldface denotations indicate the direct relatives of D7. The A-, B-, and D-series variants were generated by random mutagenesis while C-series by DNA shuffling.

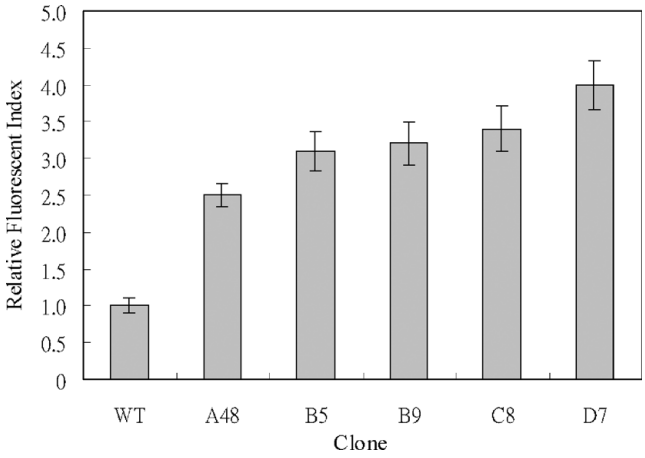


Fig. 2. Relative fluorescent intensities of D7 and its direct progenitors. Fluorescent intensity was measured from BL21(DE3) transformants expressing wild type BfgV (WT), D7, or D7's direct progenitors. The data are transformed into relative fluorescent index. The error bars indicate the standard deviation.

### *Sequence analysis*

DNA sequences of all the *bfgV* mutants selected from each round were determined and compared. The average mutation frequency caused by error-prone PCR was 0.66%. There were totally 21 base changes in *D7* mutant gene and its direct progenitors. Twenty of them originated from error-prone PCR and the remaining one from shuffling procedure. Eight of the 12 DNA mutations in *D7* resulted in amino acid substitutions. To confirm if all the eight substitutions (E40K, V76A, L77I, V83M, S124C, T171M, G176S, and E179K) were indeed critical for conferring the elevated fluorescence of D7 mutant protein, each of them was independently reverted to wild genotype by site-directed mutagenesis [26]. The FI values of all the revertants decreased over 65% that of D7 with the exception of T171M revertant that showed a similar FI value as D7. Therefore, E40K, V76A, L77I, V83M, S124C, G176S, and E179K were the effective substitutions in D7 mutant protein.

### *Fluorescent difference between BfgV and D7 mutant*

*Escherichia coli* hosts harboring *D7* mutant gene showed a slightly different fluorescent color. When analyzed by fluorometer, BL21(DE3)/pD721 transformants exhibited an emission peak at 440 nm which was 16 nm shorter than that of BL21(DE3)/pFP21. However, their excitation maxima were similar to each other (Fig. 4).

### *3D structure modeling of BfgV*

Sequence analysis indicated that BfgV could be classified into the short-chain dehydrogenase/reductase (SDR) superfamily [27–29]. Therefore, a

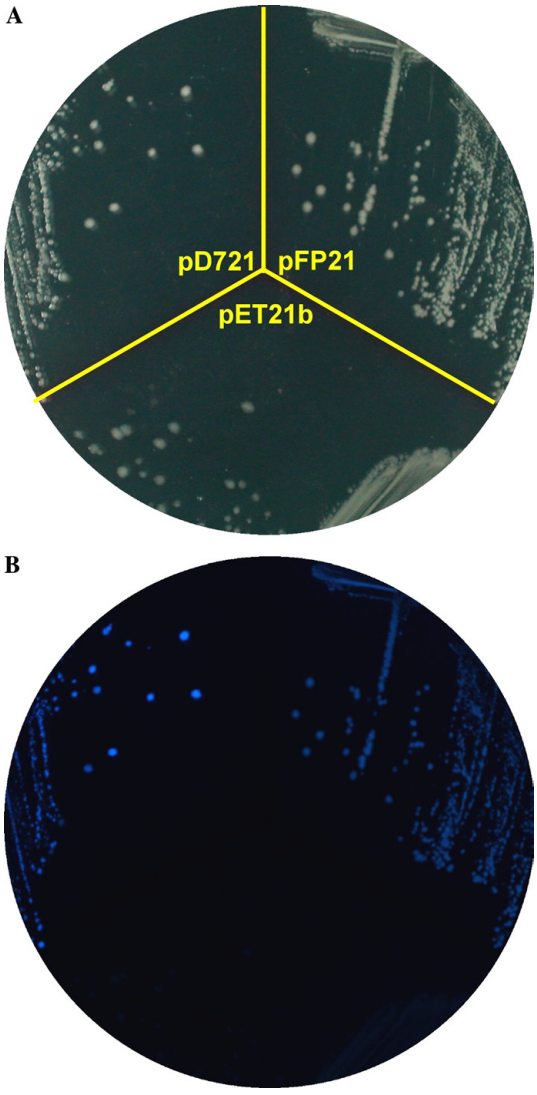


Fig. 3. Fluorescence of transformed *E. coli* cells expressing BfgV or its mutant D7. *E. coli* BL21(DE3) cells transformed with pFP21 (carrying *bfgV*), pD721 (carrying *D7*) or pET21b were grown at 37 °C for 16 h on a LB agar plate supplemented with ampicillin and IPTG. Photographs show transformed colonies illuminated with (A) white light; (B) 365 nm ultraviolet. The BL21(DE3)/pET21b was used as a negative control.

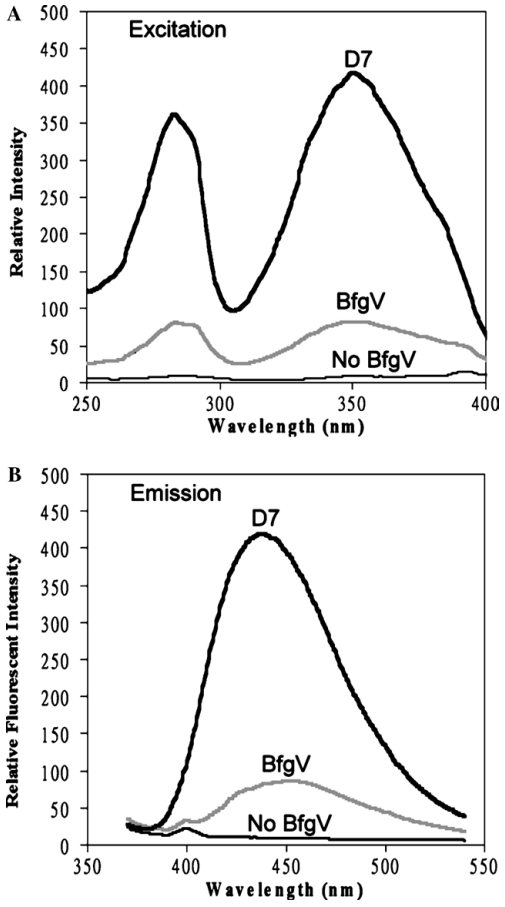


Fig. 4. Comparison of the fluorescent spectra of BfgV and D7 mutant protein. The excitation and emission spectra of D7 and BfgV in BL21(DE3) transformants were determined. (A) Two excitation peaks of BfgV and D7 are all at 283 and 352 nm. (B) The emission peak of D7 is at 440 nm while BfgV at 456 nm. The spectra curves of negative control, BL21(DE3)/pET21b, are also showed and designed as "no BfgV."

structure-established SDR member, meso-2,3-butanediol dehydrogenase (m-BD) [22], was applied as a template for modeling BfgV structure. The m-BD shares 31% residue identity with BfgV. Partial 3D structure of BfgV showing 1–194 amino acid residues was thus established on the coordinates of m-BD structure by the modeling program in Swiss-Model server (Fig. 5).

*Protein synthesis and fluorescent formation of D7*

Fluorescence of GFP relies on a specific fluorophore. The formation of this structure is oxygen-dependent. However, the fluorescence of BfgV and its derived mutants comes from NADPH binding. To clarify if there was any difference between protein synthesis and fluorescent formation in vivo, BL21(DE3)/p19D7 and BL21(DE3)/pGFP transformants were cultured and then analyzed. Time course analysis clearly showed the fluorescence of wild type GFP significantly fell behind GFP synthesis, but the protein synthesis and fluorescence appearance of D7 looked synchronic (Fig. 6). The "synchronic" property of D7 suggested NADPH bound to this protein as soon as it was synthesized in cells.

## Discussion

In this study, BfgV protein of *V. vulnificus* CKM-1 was successfully evolved to increase its fluorescent intensity. Its first mutant A48 made the most obvious jump in this property when all candidates selected from different stages were inspected. This mutant protein contained

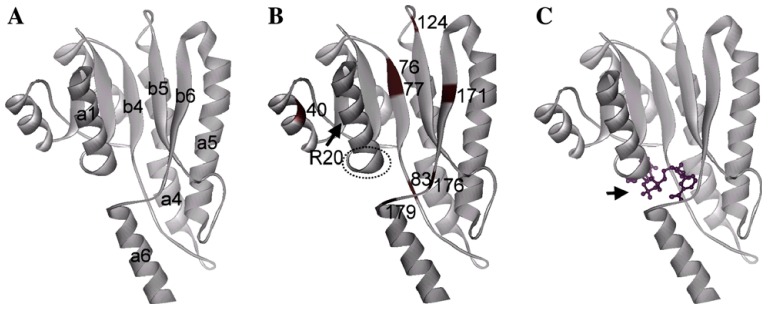


Fig. 5. The eight amino acid substitutions of D7 on the partial 3D structure of BfgV. This modeled structure is composed of 1–194 amino acid residues of BfgV according to the coordinates of m-BD. (A) The relative positions of some secondary structures of BfgV are showed on the modeled structure. a, α-helix; b, β-strand. (B) Positions of the eight substitution sites, E40K, V76A, L77I, V83M, S124C, T171M, G176S, and E179K, are labeled on the 3D structure of BfgV and darkly marked. An arrowhead denotes the site of residue R20 and dashed circle the motif $Gly^{9}XXXGly^{13}XGly^{15}$. (C) The possible binding manner of NADPH on BfgV protein is showed. An arrowhead indicates NADPH in the cleft of BfgV with its nicotinamide ring outward.

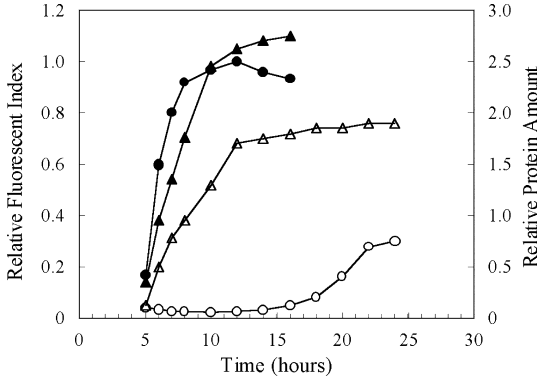


Fig. 6. The kinetics of protein synthesis and fluorescence formation of D7 and wild type GFP in vivo. BL21(DE3)/p19D7 or BL21(DE3)/pGFP transformants were grown at 37 °C in LBA broth with 200 rpm shaking. Samples were taken at specific time points. An equal amount of cells taken from each sample was applied to SDS–PAGE for protein analysis. Relative FI of each sample was also determined. The excitation and emission wavelengths were (352, 440 nm) for D7 and (395, 509 nm) for GFP. The legends used in this figure are: D7 protein (▲); D7 fluorescence (●); GFP protein (△); and GFP fluorescence (○).

only one G176S substitution. Therefore, this mutation should be important to the fluorescent elevation. This viewpoint was also supported by the fact that the C-series mutants did not lose G176S substitution even after DNA shuffling process. The best clone *D7* selected from the final round was the offspring of *C8*. The fluorescent intensity of C8 was 5% lower than that of its peer C9. This fact suggests that mediocre parents do not mean to lose the ability to generate outstanding offspring.

It is reasonable to speculate that the eight substitutions in D7 mutant protein, or at least some of them, may be close to the NADPH-binding site if they actually influence the fluorescence intensity of D7–NADPH complex. The prerequisite for knowing the locations of these amino acid substitutions is based on the knowledge of the structure feature of BfgV. As described in our previous report, BfgV belongs to the SDR superfamily [9,10]. Most members of this superfamily have highly similar 3D structures in the two-thirds parts of their polypeptide chains from N-terminal, in spite of very limited residue identities (about 15–30%) between them [27]. Jornvall et al. [27] had made a admirable demonstration. He superimposed the 3D structures of 3α/20β-hydroxysteroid dehydrogenase [30] on that of dihydropteridine reductase [31] and showed their structures are very similar although these two proteins shared only 15% residue identity. Thus, modeling a SDR protein through a well-established 3D structure of another member of this family is practicable [32]. We therefore constructed the partial 3D structure of NADPH-binding BfgV on the base of m-BD, which is also a member of the SDR superfamily. As comparing this modeled structure with those of other NADPH-binding proteins [34,35], we confirmed the common motif $Gly^{9}XXX Gly^{13}XGly^{15}$ (for phospho-diester bond) [27] and conserved amino acid residues such as $Arg^{35}$ (for 2′-phosphate) [33] and $Lys^{145}$ (for nicotinamide) [27] were all located at right positions. Therefore, this structure was reliable. When the eight substitutions identified in D7 were assigned to the modeled structure, three substitutions, V83M, G176S, and E179K, were found around the NADPH-binding site (Fig. 5). V83M substitution is close to the adenine ring of NADPH, while G176S is just beside the nicotinamide ring by which NADPH fluoresces. G176S substitution was the aforementioned critical substitution in A48 mutant and was propagated into its outstanding offspring. The effect of E179K did not seem to act directly on NADPH because the side chain of Lys is far away from NADPH molecule. An interesting thing was that these three substitutions were distributed on loop 4 (between β-strand 4 and α-helix 4) and loop 6 (between β-strand 6 and α-helix 6), whereas no mutation was found on loop 5. This seemed reasonable because loop 5 looked far away from the NADPH-binding site in the modeled 3D structure

(Fig. 5). Therefore, loop 4 and loop 6 in BfgV molecule should be the essential regions that influenced the fluorescent intensity of BfgV–NADPH complex. Besides, V76A and L77I on β-strand 4 were located just on the upstream region of loop 4 (Fig. 5). These two substitutions probably tuned the position of the downstream loop 4 through changing the side chain interactions in the β-sheet core and indirectly influenced some key residues of loop 4 to interact with NADPH. As to the E40K, a charge reverse might interrupt the ionic interaction between residue E40 and R20, and subsequently influenced an important NAD(P)H-binding motif, $Gly^{9}XXXGly^{13}XGly^{15}$, which was just under the α-helix 1 (Fig. 5) [27]. According to the reports about NAD(P)H-binding fluorescent proteins [6,8,11], the emission wavelength shift and even the increase of fluorescent intensity result from the conformational change of bound NAD(P)H [11]. We think the results of this study responded well to this theory and also proved our previous viewpoint that modification of the peptide skeleton of BfgV might increase the fluorescent intensity of BfgV–NADPH complex.

The fluorescence of BfgV and its mutants comes from NADPH binding. This molecule is a common cofactor in most living organisms whether they are aerobic or anaerobic. The ''synchronic'' property of D7 suggests that NADPH binds to this protein as soon as it is synthesized in cells. GFP and its derived mutants all require oxygen to form a special fluorophore for fluorescing [1,2,36]. The oxygen-dependent fluorophore formation obstructs the application of GFP under obligate anaerobic condition [37]. Many efforts have been made to refine the GFP. However, there seems to be little effort aiming at the improvement of cofactor-binding fluorescent proteins. Here, we demonstrated the possibility of increasing the fluorescent strength of NADPH-binding BfgV through directed evolution, and constructed a promising mutant D7 which possessed fluorescence intensity four times larger than BfgV. Moreover, D7 has two important properties that make this protein become a reporter candidate: first, the synchronicity of protein synthesis and fluorescent appearance in vivo makes D7 an ''on time'' reporter; second, this protein can theoretically fluoresce in both aerobic and anaerobic living cells only if they produce NADPH. In this study, we also identified the essential regions that influenced the fluorescence intensity of BfgV. This information may also be applied to other NAD(P)H-binding proteins to construct another kind of useful fluorescent protein.

## Acknowledgment

This work was supported by Grant (91-EC-17-A-10-S1-0013) from Department of Industrial Technology, Ministry of Economic Affairs of Taiwan.

## References

[1] B.P. Cormack, R.H. Valdivia, S. Falkow, FACS-optimized mutants of the green fluorescent protein (GFP), Gene 173 (1996) 33–38.
[2] A. Crameri, E.A. Whitehorn, E. Tate, W.P. Stemmer, Improved green fluorescent protein by molecular evolution using DNA shuffling, Nat. Biotechnol. 14 (1996) 315–319.
[3] T.T. Yang, L. Cheng, S.R. Kain, Optimized codon usage and chromophore mutations provide enhanced sensitivity with the green fluorescent protein, Nucleic Acids Res. 24 (1996) 4592–4593.
[4] S. Delagrave, R.E. Hawtin, C.M. Silva, M.M. Yang, D.C. Youvan, Red-shifted excitation mutants of the green fluorescent protein, Biotechnology 13 (1995) 151–154.
[5] R. Heim, D.C. Prasher, R.Y. Tsien, Wavelength mutations and posttranslational autoxidation of green fluorescent protein, Proc. Natl. Acad. Sci. USA 91 (1994) 12501–12504.
[6] R.Y. Hsu, H.A. Lardy, W.W. Cleland, Pigeon liver malic enzyme, V. Kinetic studies, J. Biol. Chem. 242 (1967) 5315–5322.
[7] J.R. Lakowicz, H. Szmacinski, K. Nowaczyk, M.L. Johnson, Fluorescence lifetime imaging of free and protein-bound NADH, Proc. Natl. Acad. Sci. USA 89 (1992) 1271–1275.
[8] B. Li, S.X. Lin, Fluorescence-energy transfer in human estradiol 17beta-dehydrogenase–NADPH complex and studies on the coenzyme binding, Eur. J. Biochem. 235 (1996) 180–186.
[9] C.C. Chang, Y.C. Chuang, Y.C. Chen, M.C. Chang, Bright fluorescence of a novel protein from *Vibrio vulnificus* depends on NADPH and the expression of this protein is regulated by a LysR-type regulatory gene, Biochem. Biophys. Res. Commun. 319 (2004) 207–213.
[10] J.H. Su, Y.C. Chuang, Y.C. Tsai, M.C. Chang, Cloning and characterization of a blue fluorescent protein from *Vibrio vulnificus*, Biochem. Biophys. Res. Commun. 287 (2001) 359–365.
[11] S.F. Velick, Fluorescence spectra and polarization of glyceraldehyde-3-phosphate and lactic dehydrogenase coenzyme complexes, J. Biol. Chem. 233 (1958) 1455–1467.
[12] M.E. Black, T.G. Newcomb, H.M. Wilson, L.A. Loeb, Creation of drug-specific herpes simplex virus type 1 thymidine kinase mutants for gene therapy, Proc. Natl. Acad. Sci. USA 93 (1996) 3525–3529.
[13] D.W. Leung, E. Chen, D.V. Goeddel, A method for random mutagenesis of a defined DNA segment using a modified polymerase chain reaction, Technique 1 (1989) 11–15.
[14] J.A. Wells, M. Vasser, D.B. Powers, Cassette mutagenesis: an efficient method for generation of multiple mutations at defined sites, Gene 34 (1985) 315–323.
[15] O. Kuchner, F.H. Arnold, Directed evolution of enzyme catalysts, Trends Biotechnol. 15 (1997) 523–530.
[16] K. Chen, F.H. Arnold, Tuning the activity of an enzyme for unusual environments: sequential random mutagenesis of subtilisin E for catalysis in dimethylformamide, Proc. Natl. Acad. Sci. USA 90 (1993) 5618–5622.
[17] L. You, F.H. Arnold, Directed evolution of subtilisin E in *Bacillus subtilis* to enhance total activity in aqueous dimethylformamide, Protein Eng. 9 (1996) 77–83.
[18] W.P. Stemmer, Rapid evolution of a protein in vitro by DNA shuffling, Nature 370 (1994) 389–391.
[19] J.H. Zhang, G. Dawes, W.P. Stemmer, Directed evolution of a fucosidase from a galactosidase by DNA shuffling and screening, Proc. Natl. Acad. Sci. USA 94 (1997) 4504–4505.
[20] J.C. Moore, F.H. Arnold, Directed evolution of a *para*-nitrobenzyl esterase for aqueous-organic solvents, Nat. Biotechnol. 14 (1996) 458–467.
[21] W.P. Stemmer, DNA shuffling by random fragmentation and reassembly: in vitro recombination for molecular evolution, Proc. Natl. Acad. Sci. USA 91 (1994) 10747–10751.

[22] M. Otagiri, G. Kurisu, S. Ui, Y. Takusagawa, M. Ohkuma, T. Kudo, M. Kusunoki, Crystal structure of meso-2,3-butanediol dehydrogenase in a complex with Nad(+) and inhibitor mercaptoethanol at 1.7 A resolution for understanding of chiral substrate recognition mechanisms, J. Biochem. (Tokyo) 129 (2001) 205–211.
[23] N. Guex, M.C. Peitsch, SWISS-MODEL and the Swiss-Pdb-Viewer: An environment for comparative protein modeling, Electrophoresis 18 (1997) 2714–2723.
[24] M.C. Peitsch, ProMod and Swiss-Model: Internet-based tools for automated comparative protein modeling, Biochem. Soc. Trans. 24 (1996) 274–279.
[25] T. Schwede, J. Kopp, N. Guex, M.C. Peitsch, SWISS-MODEL: an automated protein homology-modeling server, Nucleic Acids Res. 31 (2003) 3381–3385.
[26] S.N. Ho, H.D. Hunt, R.M. Horton, J.K. Pullen, L.R. Pease, Site-directed mutagenesis by overlap extension using the polymerase chain reaction, Gene 77 (1989) 51–59.
[27] H. Jornvall, B. Persson, M. Krook, S. Atrian, R. Gonzalez-Duarte, J. Jeffery, D. Ghosh, Short-chain dehydrogenases/reductases (SDR), Biochemistry 34 (1995) 6003–6013.
[28] Y. Kallberg, U. Oppermann, H. Jornvall, B. Persson, Short-chain dehydrogenases/reductases (SDRs), Eur. J. Biochem. 269 (2002) 4409–4417.
[29] B. Persson, M. Krook, H. Jornvall, Characteristics of short-chain alcohol dehydrogenases and related enzymes, Eur. J. Biochem. 200 (1991) 537–543.
[30] D. Ghosh, Z. Wawrzak, C.M. Weeks, W.L. Duax, M. Erman, The refined three-dimensional structure of 3 alpha, 20 beta-hydroxysteroid dehydrogenase and possible roles of the residues conserved in short-chain dehydrogenases, Structure 2 (1994) 629–640.
[31] K.I. Varughese, M.M. Skinner, J.M. Whiteley, D.A. Matthews, N.H. Xuong, Crystal structure of rat liver dihydropteridine reductase, Proc. Natl. Acad. Sci. USA 89 (1992) 6080–6084.
[32] M. Krook, D. Ghosh, W. Duax, H. Jornvall, Three-dimensional model of NAD(+)-dependent 15-hydroxyprostaglandin dehydrogenase and relationships to the NADP(+)-dependent enzyme (carbonyl reductase), FEBS Lett. 322 (1993) 139–142.
[33] M.J. Adams, G.H. Ellis, S. Gover, C.E. Naylor, C. Phillips, Crystallographic study of coenzyme, coenzyme analogue and substrate binding in 6-phosphogluconate dehydrogenase: implications for NADP specificity and the enzyme mechanism, Structure 2 (1994) 651–668.
[34] M. Fisher, J.T. Kroon, W. Martindale, A.R. Stuitje, A.R. Slabas, J.B. Rafferty, The X-ray structure of *Brassica napus* beta-keto acyl carrier protein reductase and its implications for substrate binding and catalysis, Struct. Fold Des. 8 (2000) 339–347.
[35] A. Yamashita, H. Kato, S. Wakatsuki, T. Tomizaki, T. Nakatsu, K. Nakajima, T. Hashimoto, Y. Yamada, J. Oda, Structure of tropinone reductase-II complexed with NADP+ and pseudotropine at 1.9 A resolution: implication for stereospecific substrate binding and catalysis, Biochemistry 38 (1999) 7630–7637.
[36] R. Heim, R.Y. Tsien, Engineering green fluorescent protein for improved brightness, longer wavelengths and fluorescence resonance energy transfer, Curr. Biol. 6 (1996) 178–182.
[37] D.A. Siegele, L. Campbell, J.C. Hu, Green fluorescent protein as a reporter of transcriptional activity in a prokaryotic system, Methods Enzymol. 305 (2000) 499–513.